日本地熱学会誌
第 39 巻　第 4 号（2017）
191 頁～ 201 頁

J.Geotherm.
Res. Soc. Japan
Vol. 39. No. 4（2017）
P.191 ～ P.201

論　文

Thermodynamic Analysis of Silica-Based Scale Precipitation Induced by Magnesium Ion

Motoaki Morita *, Yusuke Goto **, Shinichi Motoda *, and Toshio Fujino **

（Received 23 May 2017, Accepted 29 August 2017）

Abstract

The efficiency and maintenance of small geothermal power plants that use low-temperature hot spring water are affected by the adhesion scale. The precipitated scale samples from the binary power plant at Obama Hot Spring (Kyusyu, Japan) was analyzed and found to contain aragonite, quartz, and amorphous silica-based phases. Thermodynamic analysis revealed that aragonite, calcite, talc, sepiolite, and amorphous magnesium silicate were in supersaturated state in the geothermal water. Meanwhile, magnesium carbonate and amorphous silica were unsaturated. Mg^{2+} does not affect the precipitation of carbonate scale, and that of amorphous silica-based scale could be predicted thermodynamically after considering the influence of Mg^{2+}. Based on the chemical composition of the geothermal water supersaturated with amorphous magnesium silicate, we extended a simple method to predict the precipitation of amorphous magnesium silicate. The saturation indexes of both components are decreased by decreasing the pH and the temperature; hence, this could be used to reduce the adhesion scale at Obama Hot Spring. At the pH is ≥ 9, the precipitation of amorphous magnesium silicate should be considered, even if amorphous silica is unsaturated in the hot spring water (assuming ionic strength I = 0.1–0.2). With regard to the temperature, the precipitation risk of amorphous magnesium silicate is high at around 100 ˚C, but greatly reduced by operating the geothermal water at around 75 ˚C.

Keywords: magnesium silicate, amorphous silica, scaling, inhibitor, hot spring water

1. Introduction

In recent years, small geothermal power plants using geothermal hot water at low temperatures (hot spring water at around 100 ˚C, which could be used for bath) have been considered at various sites in Japan. However, it is difficult to predict the effect of adhesion scale on the power generation efficiency and the maintenance frequency. This hinders the financial assessment of these power plants and their construction. The first step to solve this problem is identifying the chemical species in the adhesion scale. Furthermore, thermodynamic analysis based on the chemical equilibrium theory could be used to predict mineral species. Scales based on carbonate ($CaCO_3$) and silica (amorphous silica and quartz) have been evaluated (e.g. NEDO, 2015). For the silica-based scales, metal ions such as Al^{3+} (Björke et al., 2012) and Mg^{2+} (Kitahara and Muraishi, 1978; Hauksson et al., 1995; Gunnarsson et al., 2002) are known to affect the property of the amorphous silicate, and therefore they must be considered

* Tokyo University of Marine Science and Technology, 2-1-6 Etujima, Koto-ku, Tokyo, 135-8533 Japan
** Edit Co., Ltd., 4-2-20 Tenjin, Chuo-ku, Fukuoka, 810-0001 Japan

Table 1 Chemical content of (a) water, (b) water in steam, and (c) gas in steam at Orange Bay source in Obama.

(a)Water	
Temperature, T / °C	102
pH	8.2
Electric conductivity (mS/m)	1320
Total soluble matter (ppm)	8590
Na^{+} (ppm)	2510
K^{+} (ppm)	290
Ca^{2+} (ppm)	134
Mg^{2+} (ppm)	128
Cl^{-} (ppm)	4530
SO_4^{2-} (ppm)	297
Al^{3+} (ppm)	<0.01
HCO_3^{-} (ppm)	166
F^{-} (ppm)	0.53
B^{3+} (ppm)	15.2
As^{5+} (ppm)	0.42
Total-SiO_2 (ppm)	223
δD_{H_2O} (‰)	-36
$\delta^{18}O_{H_2O}$ (‰)	-4.3

(b)Water in steam	
pH	5.3
Electric conductivity (mS/m)	20,7
Cl^{-} (ppm)	1.18
B^{3+} (ppm)	0.07
Hg (ppm)	0.002
H_2S (ppm)	6.31
NH_4^{+} (ppm)	26.9
δD_{H_2O} (‰)	-36
$\delta^{18}O_{H_2O}$ (‰)	-4.3

(c) Gas in steam		
Water-gas ratio	Mass ratio	3.3
	Volume ratio	1.39
Content	CO_2 (vol%)	97.3
	H_2S (vol%)	0.4
	R gas (vol%)	2.3

when predicting the related scale precipitation. There have many reports of aluminum silicate depositions in Japan, and the precipitation behavior of aluminum silicate has been investigated (Gallup, 1997; Nishida et al., 2009; Yokoyama et al., 1993; Yokoyama et al., 1999). Recently, the precipitation of magnesium silicate at Japanese sites has also been reported (Morita and Umezawa, 2016; Morita et al., 2017). In contrast, there are only very few reports on the precipitation condition and behavior of magnesium silicate (Ueda and Odashima, 2002). In this study, thermodynamic analysis was used to predict the dissolution and precipitation reactions of carbonate scale, silica, and magnesium silicate from the geothermal water at Obama-cho (Unzen City, Nagasaki Prefecture), where the concentration of Al^{3+} is below 0.01 ppm and hence can be ignored. We compared the prediction result with the field result from the small binary power plant located at this site, and examined the need to include magnesium silicate in the analysis. Next, the effects of pH and temperature on the dissolution and precipitation reactions were evaluated, in order to find the conditions that can best suppress scale adhesion. Finally, the concentrations of monomeric silicic acid (dissolved silica) and Mg^{2+} that could create supersaturation condition for amorphous magnesium silicate were analyzed, and an approximate method to predict its precipitation was proposed.

2. Experiment and theory

2-(1) Mineral and chemical composition of scales on power plant components

Scales adhered to the plant components at the Obama Hot Spring binary power plant from April 1 to July 17, 2013 were sampled and analyzed. Figure 1 shows the schematic diagram of the geothermal fluid transport system. The two-phase geothermal fluid gushed from the source was aerated at the aeration tank, then transported to the heat exchanger through the pipeline. Table 1 shows the chemical composition of the geothermal fluid before the aeration tank (Fig. 1). The sample consisted of hot water and steam in a water-gas volume ratio of 1.39 as measured by the syringe method. The water is classified as sodium-chloride type spring. Water condensed from the steam contained hydrogen sulfide and ammonia. Most of the gas in the steam was CO_2, with small amounts of

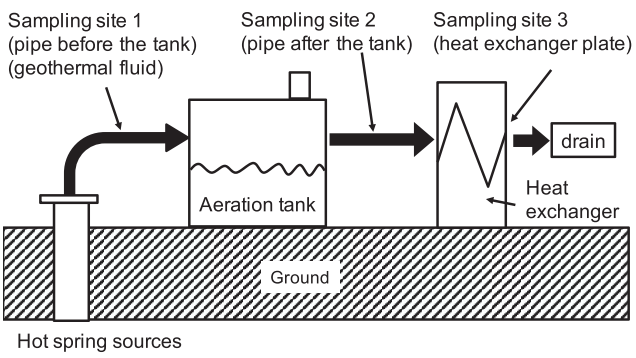

Fig. 1 Schematic illustration of the binary power plant system, and the representative sampling sites.

H_2S and residual gas. The temperature of the geothermal hot water gushed from the ground was 102 ˚C, and its pH was 8.2. Scales were found to adhere in the pipes connecting both sides of the aeration tank and on the heat exchanger through which the geothermal fluid flows (Fig. 2).

The scale samples from these locations were pulverized to about 200 μm in size with a pulverizer, and their chemical compositions were analyzed with an X-ray fluorescent (XRF) apparatus. The molar concentrations of elements heavier than Na were measured. The precipitated crystalline mineral phases were identified by an X-ray diffractometer (XRD). The chemical composition of geothermal fluid containing steam and hot water before the aeration tank source was also analyzed.

2-(2) Saturation index

The mineral phases analyzed are calcite, aragonite, magnesium carbonate, crystalline silica (quartz), amorphous silica, crystalline magnesium silicates (talc and sepiolite), and amorphous magnesium silicate. The precipitation possibility of each phase was evaluated by the saturation index (*SI*), which is represented by Eq. (1).

$$SI = \log_{10}\left(Q / K\right) \tag{1}$$

where K is the solubility product of the minerals, and Q is the ion activity product (IAP) in the geothermal fluid. A mineral phase is supersaturated in the geothermal fluid when $SI > 0$, at saturation equilibrium when $SI = 0$, and unsaturated when $SI < 0$. To account for the individual activity coefficients of the charged aqueous species, the B-dot Debye-Hückel equation designed for NaCl solutions (Eq. (2)) was used

$$\log \gamma_i = -\frac{AZ_i^2\sqrt{I}}{1+\text{å}B\sqrt{I}} + \dot{B}I \tag{2}$$

where γ_i and Z_i are the activity coefficient and charge of ion species i, I is the ionic strength, and å is an ion size parameter. The values of A and B were taken from the temperature-dependent parameters by Helgeson and Kirkham (1974). Those of å and $\dot{B}$ were taken from the parameters by Arnórsson et al. (1982) and Helgeson (1969), respectively.

2-(3) Dissolution and precipitation reactions of mineral phases

2-(3)-1) Dissolution equilibria of carbonate minerals

The dissolution and precipitation reaction of calcium carbonate is represented by Eq. (3),

$$CaCO_3\left(\text{s, } \textit{cystalline}\right) \rightleftarrows Ca^{2+} + CO_3^{2-} \tag{3}$$

while the dissociation reactions of carbonic acids are expressed as Eqs. (4)–(5).

$$H_2CO_3 \rightleftarrows HCO_3^- + H^+ \tag{4}$$

$$HCO_3^- \rightleftarrows CO_3^{2-} + H^+ \tag{5}$$

The solubility products of calcite ($K^{calcite}$) and aragonite ($K^{aragonite}$), the first acidity constant ($K_1^{CO_2}$), and the second acidity constant ($K_2^{CO_2}$) were adapted from Plummer et al. (1982). To consider the effect of Mg^{2+} on the carbonate scale, magnesium carbonate was considered for the magnesium carbonate scale. The dissolution and precipitation reactions are expressed as Eq. (6).

$$MgCO_3(\text{s}, \textit{cystalline}) \rightleftarrows Mg^{2+} + CO_3^{2-} \tag{6}$$

We used the solubility products of magnesium carbonate (K^{MgCO_3}) developed by Arnórsson et al. (1982).

2-(3)-2) Dissolution equilibria of silica-based scale

The dissolution and precipitation reactions of quartz and amorphous silica are represented by Eqs. (7)–(8).

$$SiO_2\left(\text{s, } \textit{amorphous}\right) + 2H_2O \rightleftarrows Si\left(OH\right)_4\left(aq\right) \tag{7}$$

$$SiO_2\left(\text{s, } \textit{crystalline}\right) + 2H_2O \rightleftarrows Si\left(OH\right)_4\left(aq\right) \tag{8}$$

The monosilicic acid in the solution is ionized, and the reactions can be expressed by Eqs. (9)–(10).

$$H_4SiO_4^0 \rightleftarrows H_3SiO_4^- + H^+ \tag{9}$$

$$H_3SiO_4^- \rightleftarrows H_2SiO_4^- + H^+ \tag{10}$$

The solubility products of amorphous silica (K^{AS}) and quartz (K^{Quartz}) developed by Gunnarsson et al. (2000), and the first and second acidity constants ($K_1^{Si(OH)_4}$ and $K_2^{Si(OH)_4}$) developed by Gunnarsson et al. (2000) were used. Their temperature-dependent functions can be adapted at 0–350 ˚C.

To evaluate the effect of Mg^{2+} on the precipitation of silica-based scale, three kinds of magnesium silicate were chosen: talc ($Mg_3Si_4O_{10}(OH)_2$), sepiolite ($Mg_4Si_6O_{15}(OH)_2(OH_2)_2 \cdot 4H_2O$), and amorphous magnesium silicate. Hauksson et al. (1995) reported $MgSiO_3 \cdot H_2O$ as the amorphous magnesium silicate with Mg/Si ratio = 0.77-1.0. In previous studies, the Si/Mg ratio of amorphous magnesium silicate in the scale at Obama hot spring water was found to be around 0.5-0.8 (Morita and Umezawa, 2016; Morita et al., 2017). Since the magnesium content in the scale in this case is high, the amorphous magnesium silicate was assumed to

be $MgSiO_3 \cdot H_2O$. The dissolution and precipitation reactions of talc, sepiolite, and amorphous magnesium silicate are represented by Eqs. (11)–(13), respectively.

$$Mg_3Si_4O_{10}(OH)_2(s,\ crystalline) + 4H_2O + 6H^+ \rightleftarrows 3Mg^{2+} + 4Si(OH)_4 \quad (11)$$

$$Mg_4Si_6O_{15}(OH)_2(OH_2)_2 \cdot 4H_2O(s,\ crystalline) + H_2O + 8H^+ \rightleftarrows 4Mg^{2+} + 6Si(OH)_4 \quad (12)$$

$$MgSiO_3 \cdot H_2O\ (s, amorphous) + H_2O \rightleftarrows Mg^{2+} + H_3SiO_4^- + OH^- \quad (13)$$

The solubility products of talc (K^{talc}) and sepiolite ($K^{sepiolite}$) by Gunnarson et al. (2005) were used, and these values as temperature-dependent functions are applicable at 0–350 ˚C. The solubility product of amorphous magnesium silicate (K^{AMS}) by Hauksson et al. (1995) was used. The temperature-dependent function is valid at 60–120 ˚C and extrapolated in this study to 0–60 ˚C.

3. Results and discussion

3-(1) Mineral phases adhered to the components at binary power plant

The adhesion scale found before the aeration tank has different morphology and chemical composition from that after the tank (Fig. 2 and Table 2). The pipe before the tank contained thick, white, and hard adhered scales (Fig. 2 (a)), in which the main element was Ca with small amounts of Si and Mg. Aragonite, quartz, and amorphous phase were detected in it according to the XRD analysis (Fig. 3(a)). In contrast, the scale found adhering to the pipe after the aeration tank was yellowish white and thinner than that before the tank (Fig. 2 (b)). In addition, the scale was soft and crumbled under low compression stress. The broad XRD peaks indicate that this scale mostly consisted of amorphous substances. However, the identification of individual phases was difficult due to the small number of peaks (Fig. 3 (b)). The main elements in this scale were Si and Mg. Therefore, the sample from the pipe after the aeration tank is an amorphous silica-based scale. The scale adhered to the plate in the heat exchanger is mossy in appearance (Fig. 3(c), (d)), and its chemical composition and XRD diffraction peaks are almost the same as those on the pipe after the aeration tank. In this aerated geothermal hot water utilization environment, the heat exchange had no influence on the color, chemical composition, or precipitation phase of the adhesion scale.

Table 2 Chemical compositions (mol%) of the scales adhered on (a) the pipe before aeration tank, (b) that after aeration tank, and (c) heat exchanger plate. Their photographs are shown in Fig. 2.

	Ca	Si	Mg	Fe	Mn	Al	Other
(a)	36.59	0.31	0.36	0.13	0.34	0.04	0.54
(b)	0.32	26.84	20.4	0.75	0.94	<0.02	1.35
(c)	0.18	28.29	11.35	5.06	2.59	0.03	1.03

(mol%)

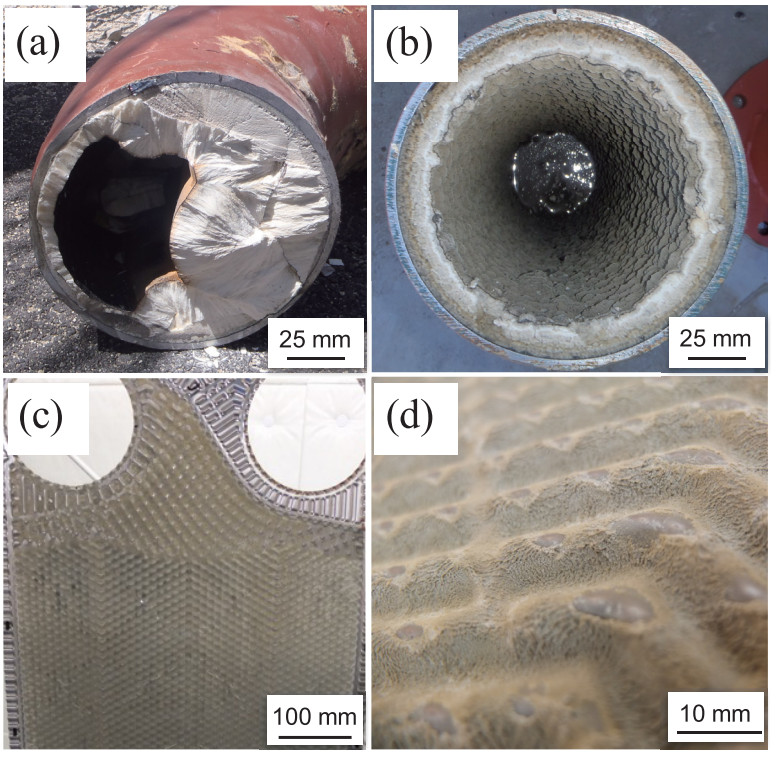

Fig. 2 Photographs of scale samples found adhered on (a) the pipe before the tank, (b) that after the tank, (c) the heat exchanger plate. (d) is the magnified photograph of the surface on the heat exchanger plate.

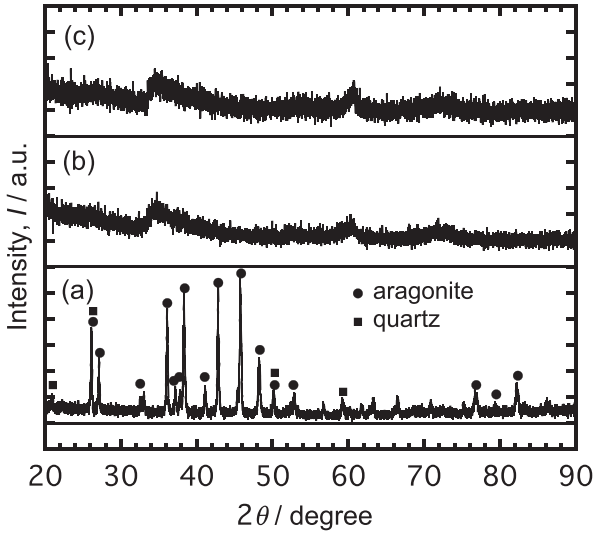

Fig. 3 XRD profiles of scales adhered on (a) the pipe before the tank, (b) that after the tank, and (c) the heat exchanger plate.

3-(2) Saturation states of mineral phases in geothermal water of Obama Hot Spring

Figure 4 shows the relationship between *SI* and the temperature based on the chemical composition of the geothermal fluid. At the temperature of the water (T = 102 ˚C), calcite, aragonite, quartz, talc, sepiolite, and amorphous magnesium silicate were in supersaturated states (*SI* = 1.76, 1.66, 0.53, 21.05, 16.48, and 4.09, respectively), while magnesium carbonate and amorphous silica were unsaturated (*SI* = -17.81 and -0.34, respectively). The field study found aragonite, quartz, and amorphous silica-based in the precipitated scales. The two polymorphs of $CaCO_3$, namely calcite and aragonite, had similar *SI* values, both being in the supersaturated state. However, only aragonite was found to precipitate in the actual environment. $CaCO_3$ polymorphs precipitated from calcium bicarbonate solution at T = 60-100 ˚C was experimentally found to be almost all aragonite according to Kitano (1964). When Mg content in the solution was around 70 ppm, however, the same study found that polymorphs other than aragonite can easily precipitate. Although that solution condition is similar to the geothermal water in this study, only aragonite precipitated from the geothermal water. Therefore, other factors must be taken into account. It may be mainly related to the rate at which CO_2 gas is lost from the hot spring water into the air, because aragonite precipitates mainly at the parts where the loss rate of CO_2 gas is fast, and calcite precipitates at the parts where this rate is slow (Kitano, 1964). Therefore, a kinetic analysis is necessary for accurately predicting the ratio between the two precipitated polymorphs. Quartz and amorphous silica-based scale precipitated in the pipe before the aeration tank, and the latter also precipitated in that after the tank. In the geothermal hot water at Obama, amorphous silica is unsaturated while amorphous magnesium silicate is in supersaturated state. Therefore, the precipitated amorphous silica-based scale is assigned to the latter. This is confirmed by the molar chemical composition of the actual sample, in which the Mg content is more than one third that of Si. Thus, it is necessary to consider the precipitation of amorphous magnesium silicate. Quartz in the supersaturated state was found to precipitate in the pipe before the aeration tank. After the aeration tank, the XRD background from the amorphous substances was high, and it was impossible to confirm the precipitation of quartz (Fig. 3). Talc and sepiolite were in the supersaturated state in the geothermal water, although their presences also could not be confirmed in the scale sample. The above results indicate that, although talc and sepiolite are in the supersaturated state, amorphous magnesium silicate (i.e., the metastable phase of magnesium silicate) first precipitates and is scarcely transformed into the crystalline form. The general temperature and pH in the water after the aeration tank are 80–105 ˚C and 8.0–8.5, respectively. When the precipitation tendencies of all mineral phases were examined, there was no significant difference among their conditions (Figs. 4–5).

3-(3) Methods to inhibit scale adhesion by temperature and pH control

The prediction of adhesion scales discussed above could effectively help finding treatment methods to suppress scale formation from the geothermal fluid. Typical treatment methods include pH adjustment (e.g. Ueda et al., 2003), CO_2 partial pressure control (e.g. Awaya et al., 1984), retention method (e.g. Nishiyama, 1981), seeded circulation method (e.g. Kato et al., 2002), and suppressing the polymerization of silica (e.g. Hosoi et al., 1982). In addition, temperature control (i.e., heating or cooling the geothermal hot water by burning waste materials or leaving the water at aeration tank) is expected to inhibit the adhesion scales. In this section, we evaluate the effectiveness of pH adjustment and temperature control at Obama Hot Spring. Figure 4 shows the dependence of *SI* of different mineral phases on temperature. The temperature conditions at which the mineral phases do not precipitate at the binary power plant are as follows: calcite: *none*, aragonite: *none*, magnesium carbonate: 0–150 ˚C, quartz: *none*, amorphous silica: > 57 ˚C, talc: *none*, sepiolite: *none*, and amorphous magnesium silicate: < 20 ˚C. In other words, calcite, aragonite, quartz, talc, and sepiolite

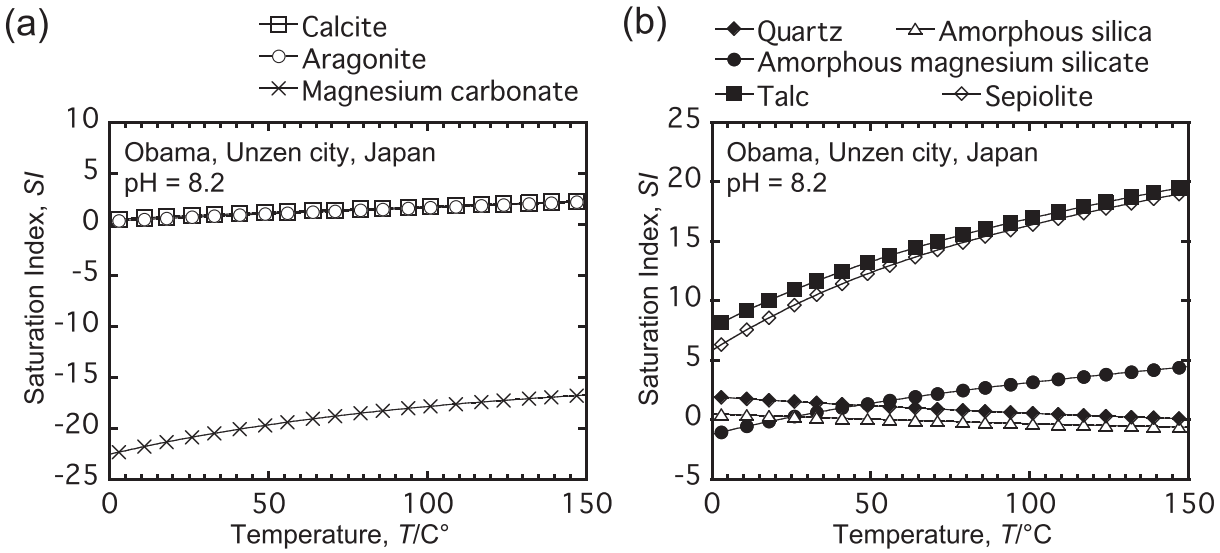

Fig. 4 Dependence of saturation index (*SI*) on the temperature for (a) carbonate scales and (b) silica-based scales at pH = 8.2 in the hot spring water from Obama, Unzen City, Japan.

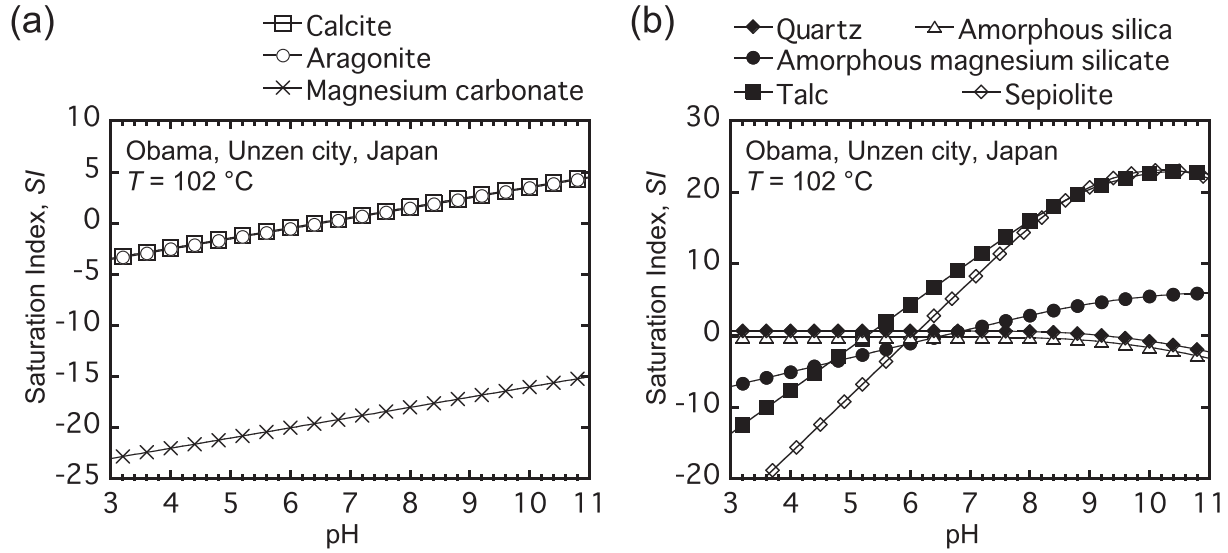

Fig. 5 Dependence of *SI* on the pH for (a) carbonate scales and (b) silica-based scales at T = 102 ˚C in the hot spring water from Obama, Unzen City, Japan.

remain saturated or supersaturated throughout the temperature range studied here. As the temperature decreases, aragonite, calcite, magnesium carbonate, talc, sepiolite, and amorphous magnesium silicate tend to dissolve, while amorphous silica and quartz tend to precipitate. Figure 5 shows the dependence of *SI* of various mineral phases for pH = 3–11: the unsaturated conditions were calcite (< 6.5), aragonite (<6.6), magnesium carbonate (3–11), quartz (> 9.2), amorphous silica (3–11), talc (< 5.3), sepiolite (< 6.1), and amorphous magnesium silicate (< 6.6). At any given pH value within the studied range, one or more phases would precipitate. The precipitation of $CaCO_3$ is sensitive to pH change, and it tends to dissolve as pH decreases. Quartz and amorphous silica are also sensitive to pH when pH > 9.0. Magnesium silicate is insensitive to pH change in alkaline solutions (pH > 9.0), but becomes sensitive when pH < 9.0. In terms of both temperature and pH, the precipitation tendency of magnesium silicate is the reverse to that of silica. Mg^{2+} did not affect the precipitation of carbonate minerals.

The main mineral phases found in the adhesion scale in the field environment were aragonite and amorphous magnesium silicate, both of which tend to dissolve at lower

temperature and lower pH. This suggests that they can be inhibited by the same treatment. In particular, pH control should be effective, since both mineral phases are unsaturated at pH < 6.3. We consider the desirable hot water operating conditions at the power plant using the temperature-pH diagram in Fig. 6. In this figure, the gray area corresponds to the supersaturated state. There was no condition where none of the mineral phases precipitate in the water at Obama Hot Spring. The main precipitated phases are aragonite and silica-based scale, and the amount of precipitated quartz is extremely small. This is similar to the findings at the geothermal power plants at Hatchobaru, Otake, and Sumikawa, where the main mineral phase in the scale was amorphous silica-based scale, and the amounts of quartz was very low (Hosoi et al., 1982 and Nishiyama, 1981). When only the main mineral phases are considered, they do not precipitate under the conditions of pH < 7.2 and 64 ˚C < T < 150 ˚C (Fig. 7). If the geothermal fluid is transported or heat-exchanged to satisfy this pH-temperature range, the scale adhesion should be suppressed.

3-(4) Precipitation conditions of amorphous silica and amorphous magnesium silicate

The precipitation tendencies of amorphous silica and magnesium silicate are completely different, as shown in Fig. 6. In order to easily judge the chemical composition of the geothermal fluid in which magnesium silicate precipitates, the effect of Mg^{2+} content on the precipitation tendency of amorphous silica-based scale was investigated at pH = 7, 8,

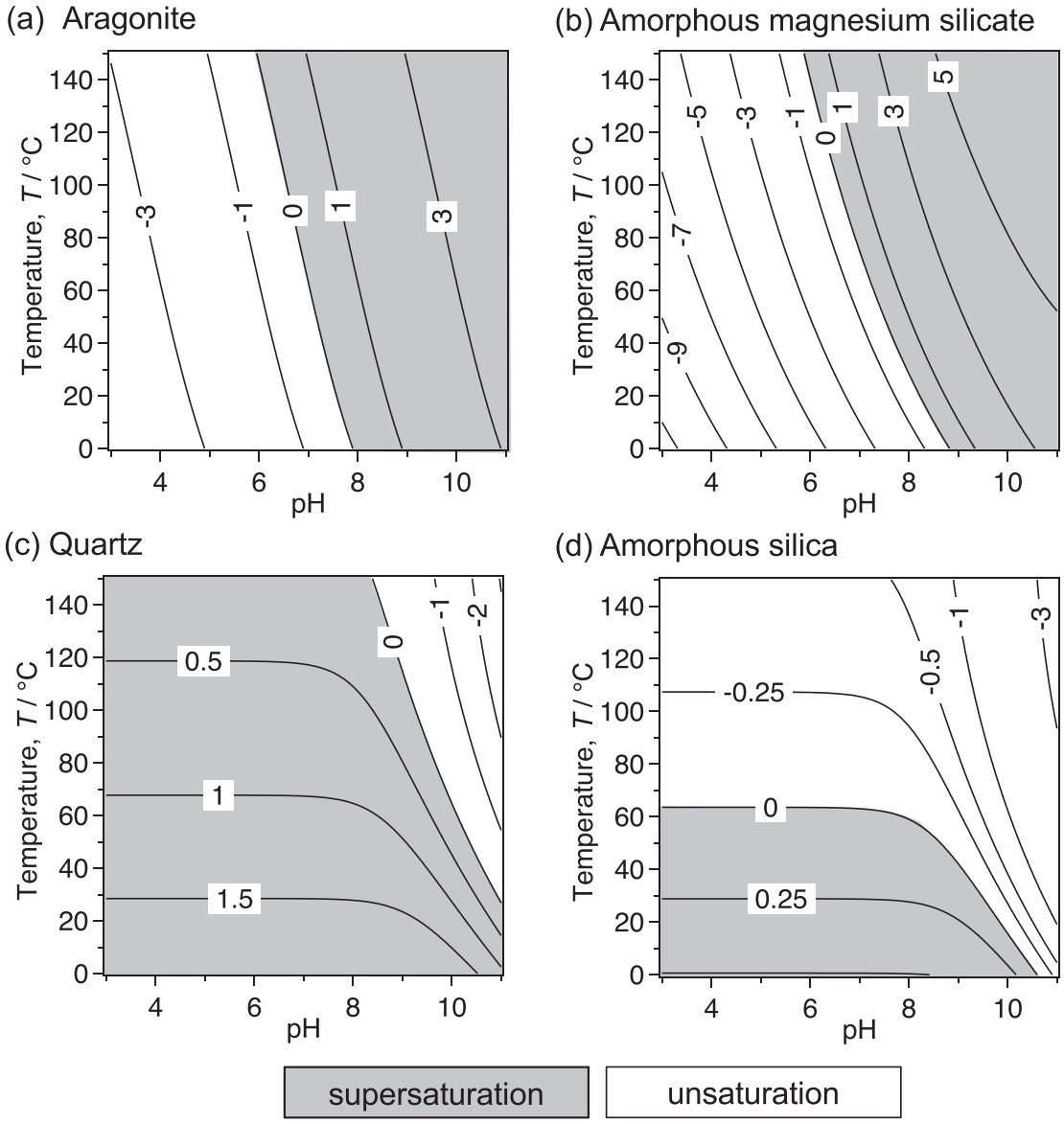

Fig. 6 Relationship among saturation index (*SI*), temperature, and pH for (a) aragonite, (b) amorphous magnesium silicate, (c) quartz, and (d) amorphous silica in Obama Hot Spring water.

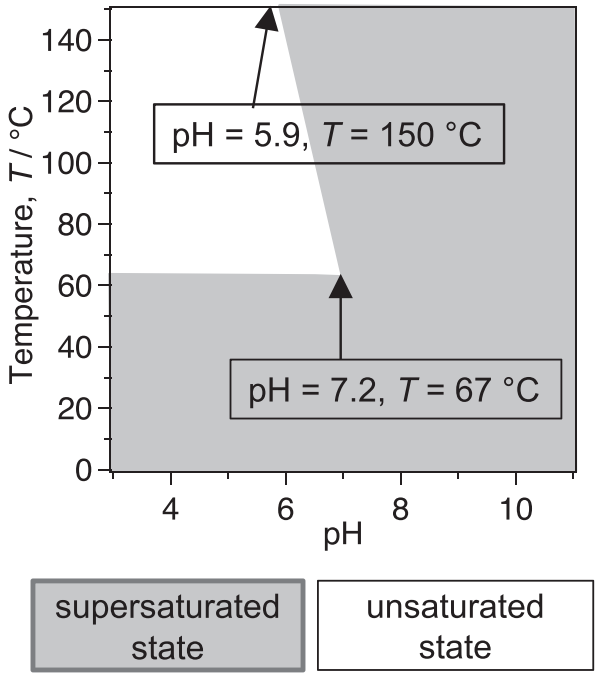

Fig. 7 Unsaturated conditions of only the main phases ($CaCO_3$ and amorphous silica-based scale).

and 9 and T = 75 and 100 ˚C. In this analysis, the chemical composition of the geothermal fluid at the binary power plant was used except for those of Mg^{2+} and dissolved silica (Fig. 8). Based on the results, we extended an approximate method originally proposed by Demadis (2010) to predict the precipitation conditions of amorphous silica and amorphous magnesium silicate in geothermal fluid (Table 3). At T > 75 ˚C and pH > 9, amorphous silica dissolves when the total dissolved silica (SiO_2) concentration is above 500 ppm, and this value is reduced by more than 50% when pH < 7. These results are in agreement with a previous study (Brown, 2011). At the conditions of T > 75 ˚C and pH > 8, even a very small amount of Mg^{2+} could promote the precipitation of amorphous magnesium silicate. Therefore, under such conditions, the precipitation of amorphous magnesium silicate should be considered, even if the total dissolved silica is less than 290 ppm in the hot spring water. When pH < 7, Mg^{2+} tends to promote the precipitation of amorphous magnesium silicate, although that of amorphous magnesium silicate is small. When pH ≥ 8, the precipitation of silica-based scale induced by Mg^{2+} becomes a problem.

In this study, the precipitation tendencies of amorphous silica and amorphous magnesium silicate were examined by thermodynamic analysis using chemical equilibrium calculation, and the necessity of accounting for amorphous magnesium silicate was shown. To facilitate the related commercial assessment by taking account of the scaling effect, it is imperative to improve the precipitation prediction methods by considering the effects of other metal ions, as well as developing related kinetic analysis techniques.

4. Conclusions

The tendency of silica-based scale precipitation induced by Mg^{2+} (magnesium silicate) was analyzed. The effects of temperature and pH on suppressing the precipitation of main mineral phases in adhesion scale were evaluated. We revealed the correlation between the amounts of dissolved silica and Mg^{2+} on forming supersaturated amorphous magnesium silicate in the geothermal hot water at Obama Hot Spring, Japan. Guidelines are proposed for the conditions under which the Mg^{2+}-induced precipitation of silica-based scale should be taken into account.

1. At Obama Hot Spring, the precipitated scale at the binary power plant consists of aragonite, quartz, and amorphous silica-based materials. Thermodynamic analysis also revealed that aragonite, calcite, talc, sepiolite, and amorphous magnesium silicate were in supersaturated state in the geothermal water, however amorphous silica was unsaturated. By considering the influence of Mg^{2+} on the precipitation of silica-based scale, the precipitation of amorphous silica-based scale could be predicted thermodynamically.
2. The main mineral component of the scale from the geothermal hot water at Obama Hot Spring was $CaCO_3$ or amorphous magnesium silicate. The saturation indexes of both components could be reduced by decreasing the pH and temperature. Adjusting these conditions should therefore be effective for suppressing the scale adhesion at the associated binary geothermal power plant.
3. Thermodynamic analysis was used to evaluate the chemical composition of geothermal water in which the adhesion of amorphous magnesium silicate occurs. At pH ≥ 9, amorphous magnesium silicate may precipitate from the geothermal water in the presence of about 1 ppm Mg. It was suggested that the risk of amorphous magnesium silicate precipitation is high near 100 ˚C, but greatly reduced by operating the geothermal water at near 75 ˚C.

Acknowledgement

These findings were the results of the project “geothermal power generation technology research and development” commissioned by the New Energy and Industrial Technology Development Organization (NEDO). The field study was performed with Hotel Orange Bay and Obama Onsen

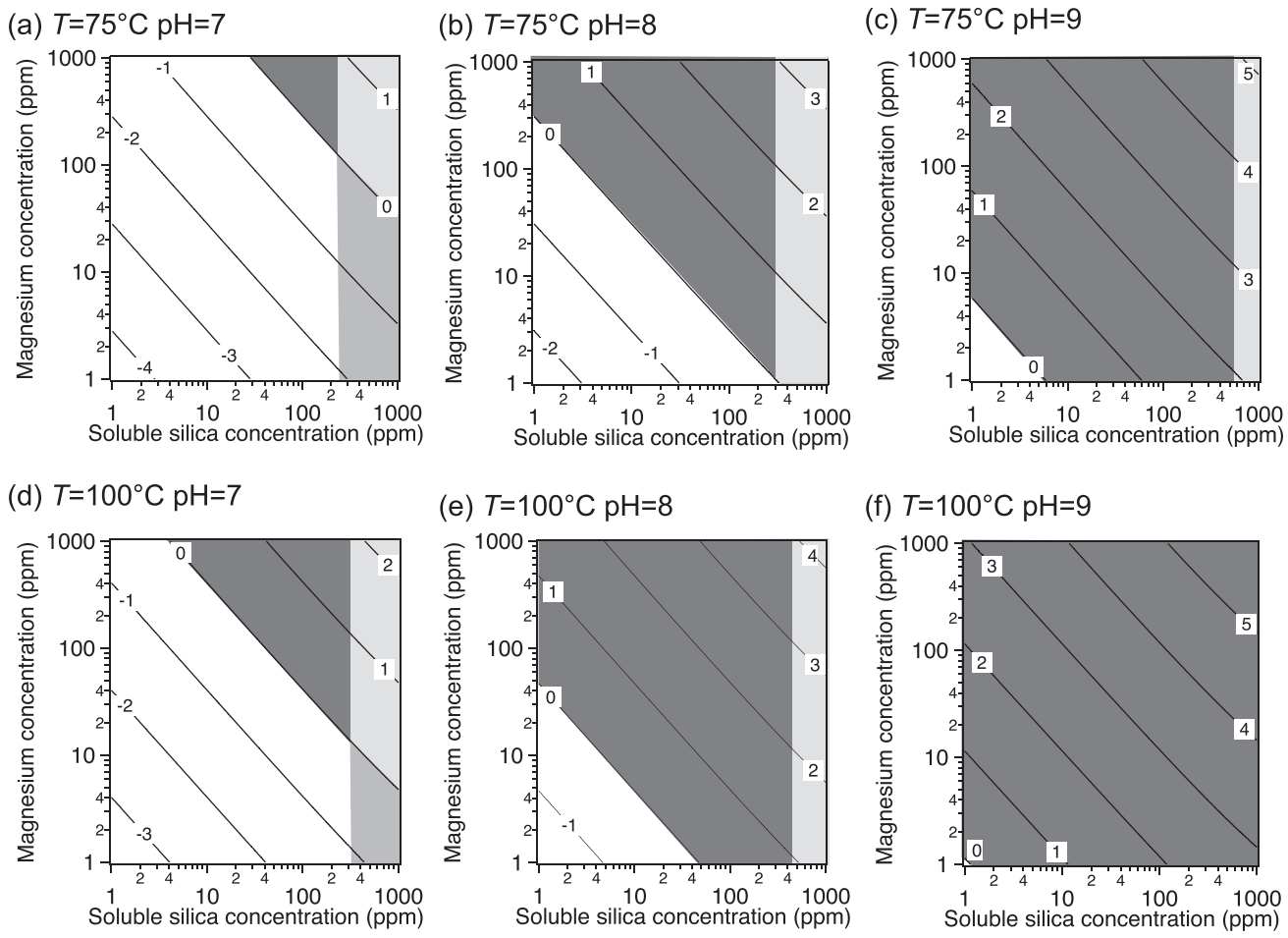

Fig. 8 Contour maps of saturation index (*SI*) for amorphous silica and amorphous magnesium silicate at T = 75 and 100 °C with pH = 7, 8, and 9.

Table 3 Predicted approximate precipitation conditions of amorphous silica and amorphous magnesium silicate. These conditions are applicable at least at ion strength I = 0.10–0.20 in the geothermal hot water. Mg and SiO_2 shown in the table are the concentrations of total soluble silica and magnesium ions in the geothermal water, respectively.

Temp.	Scale component	pH			Reference
		pH = 7	pH = 8	pH = 9	
n.d.	Amorphous silica	SiO_2 > 200 ppm	SiO_2 > 150 ppm	SiO_2 > 100 ppm	Demadis (2010)
	Amorphous magnesium silicate	Mg×SiO_2 > 40,000 ppm^2	Mg×SiO_2 > 12,000 ppm^2	Mg×SiO_2 > 3,000 ppm^2	Demadis (2010)
75 °C	Amorphous silica	SiO_2 > 260 ppm	SiO_2 > 290 ppm	SiO_2 > 550 ppm	This study
	Amorphous magnesium silicate	Mg×SiO_2 > 40,000 ppm^2	Mg×SiO_2 > 310 ppm^2	Mg×SiO_2 > 5 ppm^2	This study
100 °C	Amorphous silica	SiO_2 > 370 ppm	SiO_2 > 430 ppm	SiO_2 > 1000 ppm	This study
	Amorphous magnesium silicate	Mg×SiO_2 > 4,400 ppm^2	Mg×SiO_2 > 40 ppm^2	Mg×SiO_2 > 1 ppm^2	This study

n.d.: not defined
SiO_2 : total dissolved silica content
Mg: Mg^{2+} content

Energy. In addition, Dr. Hiroshi Kihira, Director of Technology Development, NIPPON STEEL & SUMIKIN ANTI-CORROSION CO., LTD, provided us with valuable discussions on thermodynamic analysis. We would like to express our sincere gratitude to them.

References

Arnórsson, S., Sigurdsson, S. and Svavarsson, H. (1982) The Chemistry of geothermal waters in Iceland. I. Calculation of aqueous speciation from 0 to 370 °C. Cosmochimica Acta, **46**, 1513-1532.

Awaya, T., Hirano, T. and Oki, Y. (1984) pH and partial pressure of CO_2 in subsurface thermal water. Reports of hot springs Research Institute of Kanagawa Prefecture, **15**, 65-72. *

Brown, K. (2011) Thermodynamics and kinetics of silica scaling. Proceedings of International Workshop on Mineral Scaling 2011, Manila, Philippines, 25-27 May 2011.

Björke, J.K., Mountain, B.W. and Seward, T.M. (2012) The solubility of amorphous aluminous silica: implications for scaling in geothermal power stations between 100-350°C. New Zealand geothermal workshop 2012 proceedings.

Demadis, K.D. (2010) Recent developments in controlling silica and magnesium silicate foulants in industrial water systems. In: The Science and Technology of Industrial Water Treatment (Amjad, Z. ed.), IWA publishing and CRC press, 179-204.

Gallup, D.L. (1997) Aluminum silicate scale formation and inhibition: Scale characterization and laboratory experiments, Geothermics, **28**, 483-499.

Gunnarsson, I. and Arnórsson, S. (2000) Amorphous silica solubility and the thermodynamic properties of $H_4SiO_4^0$ in the rang of 0 °C to 350 °C at P_{sat}. Geochimica et Cosmochimica Acta, **64**, 2295-2307.

Gunnarsson, I., Arnórsson, S. and Jakobsson, S. (2002) Magnesium-silicate scales in geothermal utilization. An experimental study. Science Institute Report RH-06-02, University of Iceland, 1-67.

Gunnarsson, I., Arnórsson, S. and Jakobsson, S. (2005) Precipitation of poorly crystalline antigorite under hydrothermal condition. Geochmica et Cosmochimica Acta, **69**, 2813-2828.

Hauksson, T., Prhallsson, S., Gunnlaugsson, E. and Albertsson, A. (1995) Control of magnesium silicate scaling in district heating system. Proceedings World Geothermal Congress 1995, 2487-2490.

Helgeson, H.G. and Kirkham, D.H. (1974) Theoretical prediction of the thermodynamic behavior of aqueous eectrolytes at high pressures and temperature: II. Debye-Hückel parameters for activity coefficients and relative partial moral properties. American J. Sci. **274**, 1199-1261.

Helgeson, H.G. (1969) Thermodynamics of hydrothermal systems at elevated temperatures and pressure. American J. Sci. **267**, 729-804.

Hosoi, M. and Imai, H. (1982) Study on precipitation and prevention of the silica scale from the geothermal hot water, J. Geotherm. Re. Soc. Japan, **25**, 4, 127-142.

Kato, K., Ueda, A., Mogi, K., Mori, H., and Shimojo, M. (2002) Silica removal from the geothermal brine by addition of calcium compounds in a silica treatment reactor. J. Geothermal Re. Soc. Japan, 24, 221-236.*

Kitano, Y. (1964) Geochemistry for precipitation of $CaCO_3$ in hot spring water part II. Journal of the Society of Engineers for Mineral Springs. Japan, **2**, 99-103. **

Kitahara, S. and Muraishi, H. (1978) Adsorption of soluble silica on Magnesium Hydroxide, Nippon Kagaku Kaishi, **4**, 555-560. *

Morita, M. and Umezawa, O. (2016) A model of scale formation process to inner wall carbon steel pipe for transporting hot spring water. J. Japan Inst. Met. Mater., **80**, 309-316. *

Morita, M. and Umezawa, O. (2016) A model of scale formation on inner carbon steel pipe for transporting hot spring water. Materials Transactions, **57**, 1652-1659.

Morita, M., Shinohara, W., Hashimoto, R. and Motoda, S.(2017) Microstructural analysis of initial scale formed on stainless steel sheet immersed in hot spring water. ECS trans., **75**, 9-17.

New Energy and Industrial Technology Development Organization (NEDO) and Geothermal Energy Research & Development Co., Ltd. (2015) Examination of the technical requirements concerning a downsizing, efficient-izing of the geothermal power generation system, and the binary cycle power generation using hot spring thermal energy. NEDO FY2012 Final Report (12102442-0), 86-101.

Nishida, I., Shimada, Y., Saito, T., Okaue, Y. and Yokoyama, T. (2009) Effect of aluminum on the deposition of silica scales in cooling water systems. J. Colloid and interface Science, **335**, 18-23. *

Nishiyama, H. (1981) Removal of polymerized silica from geothermal hot water by flotation. Flotation, **28**, 203-216.***

Plummer, L.N., Busenberg, E.(1982) The solubilities of calcite, aragonite and vaterite in CO_2-H_2O solutions between 0 and 90 ˚C, and an evaluation of the aqueous model for the system $CaCO_3$-CO_2-H_2O, Geochimica et Cosmochimica Acta, **46**, 1011-1040.

Ueda, A., Kato, H., Miyauchi, T. and Kato, K. (2003) Investigation of pH control method to avoid silica scaling in the Sumikawa geothermal field, J. Geotherm. Re. Soc. Japan, **25**, 163-177. *

Ueda, A. and Odajima, Y. (2002) Experimental study of stability of amorphous Mg-SiO_2 scale up to 300°C. J. Geotherm. Re. Soc. Japan, **24**, 207-213. *

Yokoyama, T., Sato, Y. Maeda, Y., Terutani, T. and Itoi, R. (1993) Siliceous deposits formed from geothermal water in Kyushu: I. The major constituents and the existing states of iron and aluminum. Geochemical Journal, **27**, 375-384.

Yokoyama, T., Sato, Y., Nakai, M., Sunahara, K. and Itoi, R. (1999) Siliceous deposits formed from geothermal water in Kyushu II.

Distribution and state of aluminum along the growth of deposits. Geochemical Journal, **33**, 13-18.

* in Japanese with English abstract

** The paper presented that the effect of CO_2 gas released from the hot spring water on the precipitation rate of $CaCO_3$ and the precipitation polymorphism.

*** The paper presented that the scaling from geothermal water was inhibited by the flotation method in the field experiment.

論　文

Mg^{2+} が誘起するシリカ系スケール析出反応の熱力学的解析

盛田元彰*，後藤優介**，元田慎一*，藤野敏雄**

概　要

小浜温泉バイナリー発電所において付着したスケール中の鉱物相を組織解析した。小浜温泉の温泉水における炭酸塩スケールとシリカ系スケールの析出傾向を熱力学的に解析した。スケール中の鉱物相と比較した結果，非晶質シリカ系スケールの析出を予測するためには，非晶質シリカだけでなく Mg^{2+} の影響を考慮した非晶質マグネシウムシリケートについても解析する必要があった。一方，炭酸塩スケールの形成には Mg^{2+} の影響はほとんど見られなかった。その解析手法を用いてスケール付着を抑制する地熱流体の輸送・熱交換の方法について考察し，非晶質マグネシウムシリケートの付着が問題となりうる熱水の化学組成を検討した。イオン強度が 0.1-0.2 程度の地熱熱水では，pH が 9 以上になると非晶質シリカは溶解傾向にあっても 1 ppm オーダーの Mg^{2+} によって非晶質マグネシウムシリケートが析出するリスクがあった。地熱熱水の温度が 100°C 近傍では非晶質マグネシウムシリケートの析出傾向は大きく，75°C 近傍で熱水運用することにより大幅にそのリスクが低減されることが示唆された。

キーワード：マグネシウムシリケート，非晶質シリカ，スケール，抑制剤，温泉水